

Electrochemical Studies on the Performance of SS316L Electrode in Electrokinetics

Jeong-Hee Choi¹, Sundaram Maruthamuthu^{1,2}, Hyun-Goo Lee¹, Tae-Hyun Ha¹, and Jeong-Hyo Bae^{1,*}

¹Smart Power Facility Research Center, Smart Grid Research Division, Korea Electrotechnology Research Institute, 70 Boolmosangil, Changwon, 641-120, Korea

²Corrosion Protection Division, Central Electrochemical Research Institute, Karaikudi, 630 006, India

(received date: 20 November 2008 / accepted date: 6 March 2009)

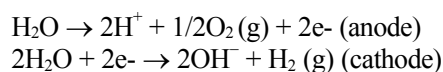
Organic and trace metal pollutants are removed by employing various electrodes in an electrokinetic (EK) process. Stainless steel was used either as an anode or a cathode by various investigators in electroremediation systems. In the present study, the role of SS316L as an anode and cathode in EK system was studied by the measurements of pH, conductivity of electrolyte, and potential of the anode and cathode at different current densities. The weight loss of the anode and cathode and the leaching of chromium, iron, and nickel at different current densities were measured and discussed with an electroosmosis process. The electrochemical behavior of SS316L electrode in neutral, acidic and alkaline pH in soil environment was studied by an electrochemical technique viz. polarization study. Surface analysis of SS316L after EK was done by XPS and SEM. The higher conductivity was noticed at anolyte when compared to catholyte. The weight loss of the anode was in the following order $0.615 > 0.307 > 0.123 \text{ mA/cm}^2$ and the cathode corrosion rate was vice versa. Peroxide production was also noticed at the anolyte, which may encourage the degradation of the total organic content (TOC) in the soil. The OCP (open circuit potential) of SS316L was about +75 mV vs SCE in the soil extract; while adding acetic acid, the potential shifted to the positive side, to about +380 mV vs SCE. The breakdown potential and the range of passivation potential were higher in acetic acid added system when compared to other systems. Pitting was observed on both the anode and cathode within 48 h during the EK process. The present study concludes that SS is not a proper electrode material for the EK process.

Keywords: electrokinetics, electrodes, SS316L, electrochemical studies, corrosion

1. INTRODUCTION

Thousands of sites are contaminated by heavy metals, organic compounds and other hazardous materials, which make an enormous impact on the quality of ground water, soil, and associated ecosystems. EK soil remediation is an emerging technology that has attracted increased interest among scientists and government officials during the last decade due to several promising laboratory and pilot scale studies and experiments. This technology aims to remove hazardous contaminants from low permeability contaminated soils under the influence of an applied direct current [1]. Electrokinetic soil treatment relies on several interacting mechanisms, including advection, which is generated by electroosmotic flow and externally applied hydraulic gradients, diffusion of the acid front to the cathode, and the migration of cations and anions toward the respective electrode

[2]. The following are the dominating reactions at the anode and cathode in an EK system.



The hydrogen ions decrease the pH near the anode. The acid front is carried toward the cathode by electrical migration, diffusion, and advection [1]. At the same time, an increase in the hydroxide ion concentration causes an increase in the pH near the cathode. Many authors have proposed that positioning the electrodes directly into the wet soil mass produces the most desirable effect [3,4]. Though seeking improvements in experiments, some researchers tend to place the electrodes not directly into the wet soil mass, but into the electrolyte solution, attached to the contaminated soil, or else to use different membranes and other materials [5,6]. In order to solubilize the metal hydroxide and carbonates formed, or different species adsorbed on the soil particles, as well as the protonate organic functional groups, there arises a necessity to introduce acid into the soil. In order to overcome

*Corresponding author: jhbae@keri.re.kr

the soil acidification of EK system from the anode compartment toward the cathode compartment (high soil-pH gradient between anode and cathode), an innovative technique has been established by the continuous addition of various acids viz. lactic acid [7], acetic acid [8, 9], nitric acid [10,11], hydrochloric acid [12], EDTA [13,14], etc. Since the organic acids have negative charges, they move toward the anode compartment [8]. Besides, sodium hydroxide is also added into the anode chamber to neutralize the acid pH of the anode compartment [15]. On the basis of utility of the electrode in the EK system, it was assumed that electrodes face three pH conditions (acidic, neutral, and alkaline) during the operation and stop-mode operation. The performance of passive electrodes has not been evaluated so far.

The electrode system is the most important part and thus considered as the heart of an EK unit. The most suitable electrodes used for research purposes are graphite [10,16] and platinum [9,17]. Virkutyte *et al.* [1] suggested that it is more appropriate to use much cheaper, reliable titanium and stainless steel for pilot studies. Stainless steel was used as an electrode material in electrokinetics by many investigators [18-23]. Alshawabkeh *et al.* [24] and Gent *et al.* [25] used stainless steel as a cathode in a pilot scale EK system. Niqui-Arroyo [26] used SS anode and cathode for removing phenanthrene. Recently, Vasudevan *et al.* [27] studied the removal of phosphate from drinking water by electrocoagulation process by employing stainless steel as the cathode. But nobody has considered the corrosion behavior of SS during EK. The authors feel that the corrosion behavior of the electrode material is also an important factor which influences the performance and efficiency of the electrokinetic system. The present study focuses on the role of SS316L on pH and electrical conductivity of electrolytes and corrosion behavior of the anode and cathode in EK system.

2. EXPERIMENTAL PROCEDURE

2.1. Electrokinetic cell configuration

Figure 1 shows a sketch of the laboratory EK reactor. The EK cell is made up of an acrylic sheet with a dimension of $24 \times 4 \times 6 \text{ cm}^3$. It is divided into three compartments. The central one is for storing the soil sample and the other two for working reservoir solution consisting of catholyte and anolyte. The air-dried soil sample was mixed with an electrolyte solution (about 30 % water content), then carefully stored in the central compartment. The length of the central compartment is 10 cm. Stainless steel 316L (SS316L) electrodes were used as the anode and cathode placed at each electrolytic compartment. To avoid soil leakage to the water reservoirs, a pair of nylon meshes [21] (mesh opening 149 μm) and a filter paper (Whatman No. 2) were placed between the soil sample and electrodes. The different current densities

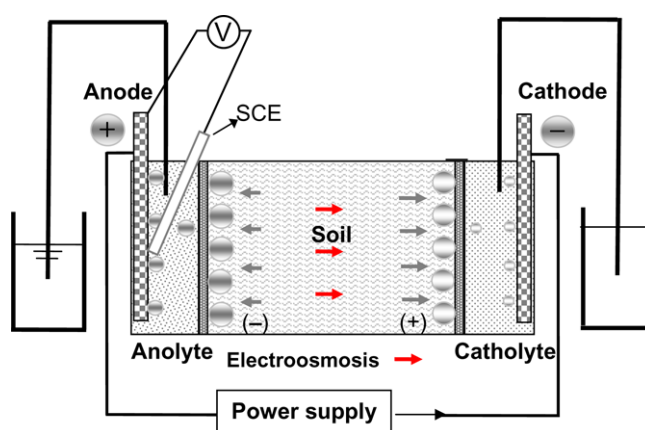


Fig. 1. Schematic diagram of EK system.

were selected viz. 0.123 mA/cm^2 , 0.308 mA/cm^2 , and 0.615 mA/cm^2 recommended by Hamed and Bhadra [28] to investigate the impact of SS316L in an EK system.

2.2. Preparation of soil extract and coupon preparation

Soil was collected from salt-contaminated soils in a greenhouse at Jinju, Gyeongangnando, and extract was taken in the ratio of 5:1 water to soil for electrochemical measurements. The original characteristics of soil used in the present study collected from Jinju are presented in Table 1. By employing the soil extract, three systems viz. acidic pH (2.40), neutral (6.9), and alkaline pH (10.30) were made with acetic acid and sodium hydroxide for the evaluation of SS316L.

Coupons of SS316L ($5 \times 2.5 \text{ cm}^2$) were used for the electrochemical study to find the corrosion behavior of the material in the above systems. The composition of SS316L is presented in Table 2. The coupons were sequentially ground with a series of grit silicon carbide papers (400, 600, 800,

Table 1. Original characteristics of soil used in the present study collected from Jinju

Soil Characteristics	Value
pH	5.6
EC (dS/m)	5.4
organic (g/kg)	25
P ₂ O ₅ , mg/kg	1384
Calcium, g/kg	3.6
Potassium, g/kg	0.9
Magnesium, g/kg	0.5
Sodium, g/kg	0.4
Nitrate, mg/kg	1878
Ammonium, mg/kg	12
Chloride, mg/kg	500

Table 2. Composition of Stainless steel 316L in percentage

Chromium	Manganese	Nickel	Carbon	Molybdenum	iron
17.2	1.6	10.9	0.02	2.1	Balance

1200, and 1500) to a smooth surface and were polished to a mirror-finish surface using different grades (0.3 micron and 0.05 micron) of alumina powders. The polished coupons were rinsed with deionized water and then the surface was cleaned by acetone and finally dried in a desiccator. The prepared coupons were used for the EK experimental studies and after completing the EK experimental studies, the coupons were used for the SEM (Scanning Electron Microscopy) and XPS (X-ray photoelectron spectroscopy) studies. Electrical leads to the coupons were made with nichrome wire and the bimetallic junction was insulated with lacquer. The same coupons were also used for electrochemical studies.

2.3. pH, conductivity, and peroxide measurements

While conducting the EK experiment at different current densities, pH, conductivity, leaching of chromium, iron and nickel, and peroxide of the electrolytes were measured. After calibration with a standard pH solution, the pH of the electrolytes was measured by a pH meter (Istek Inc., Model 76P). Electrical conductivity (EC) was measured for the electrolytes by employing EC meter (Istek Inc., Model 47 C). The average value of the two experiment samples is presented. Peroxide was measured in the anolyte and catholyte by using a test kit (Merckoquant, Peroxide test). Electroosmotic flow for a higher current density (0.615 mA/cm^2) was measured in the EK by the collection of excess electrolytes from the cathode chamber.

2.4. Estimation of leaching of electrode components

The leaching of chromium, nickel, and iron in the catholyte and anolyte at the constant current densities of 0.123 mA/cm^2 , 0.307 mA/cm^2 and 0.615 mA/cm^2 in the electrolyte were estimated for the two experiment systems. The average values are presented. The above components were estimated by an atomic absorption spectroscopy (AAS; AAnalyst 800, PerkinElmer) by the standard procedure.

2.5. Weight loss study

After finishing the EK experiments, final weights of the anode and cathode were taken and the average corrosion rates for the anodes and cathodes were calculated. The corrosion rate was calculated by the procedure recommended by NACE [29].

2.6. Scanning Electron Microscope (SEM) observation

After running the EK system for 48 h, the anode and cathode stainless steel coupons were subjected to SEM analysis. The coupons were characterized by SEM after removal of the corrosion product using 10 % nitric acid at 60°C for 15 min. SEM (Hitachi, S-4800) with a beam voltage of 15 kV was used to visualize the morphology of the surface.

2.7. Electrochemical measurements

Potential measurements during the EK process for the anode and cathode were done by using a Saturated Calomel Electrode (SCE). The reference electrode was put in the EK system nearer to the anode and cathode as mentioned in Fig. 1, and potentials were measured by employing a digital multimeter (Gold Star Model DM-311). The same coupons were immersed in different soil extract systems viz. acidic pH, neutral, and alkaline pH, and electrochemical studies were characterized by employing a potentiostat Solarton Model 1480-Multistat. OCP (Open circuit potential) measurements with time were made for the SS316L in acid, neutral, and alkaline pH systems by immersing 50 % area of the SS316L [30]. The OCP values were measured with time using a potentiostat with a commercial SCE reference electrode. Six commercial SCEs were maintained in the laboratory and calibrated against each other at least once a week. Reference electrodes were only used for the electrochemical studies when their potential was within 5 mV of the others. Thus, the potentials reported in this paper should be regarded as having an accuracy of about $\pm 5 \text{ mV}$. Anodic and cathodic polarization were conducted for the SS316L in the above systems under an air-saturated condition using a computer-controlled potentiostat in a 500 ml polarization cell. A three-electrode setup was used consisting of the test coupon as the working electrode, SCE as the reference, and a 2 cm^2 platinum gauge as the auxiliary electrode. The test coupon was first immersed in the corrosion cell for twenty minutes to allow equilibrium with the electrolyte. Cathodic polarization was initiated at the coupon OCP and polarized to -1500 mV SCE at a scan rate of 0.116 mV/s . IR drop compensation was not needed since this was a high conductivity electrolyte. Polarization was also carried out on coupons of the SS316L by a half immersion method [30]. Anodic polarization was also initiated at the coupon OCP and polarized to $+1500 \text{ mV vs SCE}$ by the above scan rate.

2.8. X-ray photoelectron spectroscopy (XPS) studies

After finishing the EK experiments, the surface of the anode and cathode was characterized by X-ray photoelectron spectroscopy (XPS). The elements on the surface film were analyzed by XPS. XPS was conducted on the surface of the electrodes using monochromatic Al $K\alpha$ radiation (VG Scientifics, ESCALAB 250). The anode voltage and power were 10 kV and 150 W, respectively. To compensate for the surface charging effect, all core level spectra were referenced to the C1s peak at 284.6 eV .

3. RESULTS AND DISCUSSION

The operational parameters and the construction of facilities are critical in the EK system. The selection of electrode materials relates not only to electrochemical reactions on the

electrode surface but also to the remediation cost. The selection of an electrode influences the efficiency and life of the EK system [31]. Since different electrode materials may induce different oxidations or reductions, various products are produced [21]. The formation of pH and conductivity depend upon the electrochemical behavior of electrodes. Oxygen reduction and evolution potentials influence the behavior of all materials on the removal of pollutants in EK. Besides, corrosion of electrolytes is also an important factor in EK. Hence, selection and evaluation of electrode material are very important aspects in the EK system.

3.1. pH and conductivity

Figures 2 and 3 show the pH and conductivity of the working solution as a function of operation time under different current densities viz. 0.123 mA/cm², 0.307 mA/cm², and 0.615 mA/cm². The pH of the anolyte and catholyte at 0.615 mA/cm²

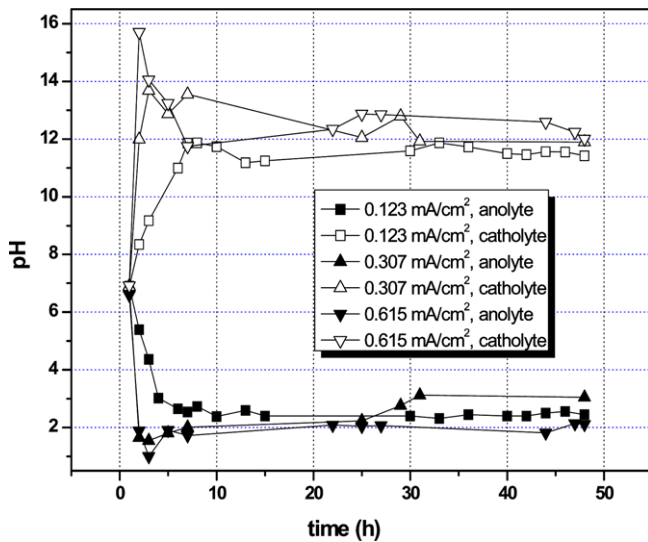


Fig. 2. pH of anolyte and catholyte in EK system.

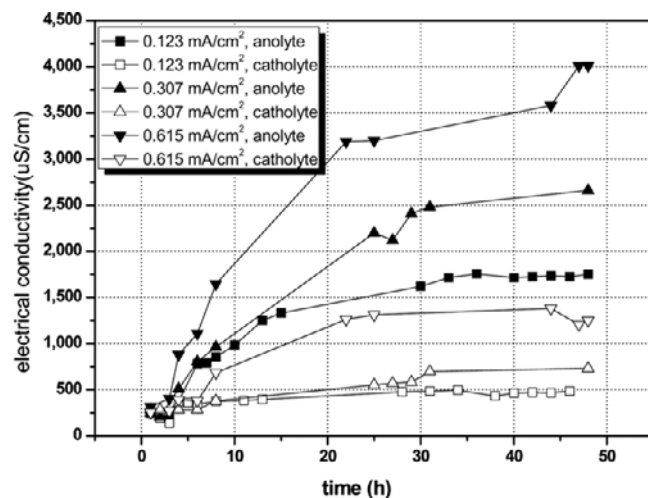


Fig. 3. Electrical conductivity of anolyte and catholyte in EK system.

increased sharply and there was no variation on pH between the current densities. The pH of the solution changed initially and gradually reached the equivalent titration point of the electrolyte. Though the reaction rate of water electrolysis is related to electrode potential, electrode surface properties, it can be concluded that electroosmosis is also an important factor on the distribution of pH at anolyte and catholyte. Higher conductivity was noticed at anolyte when compared to catholyte. It reveals that the ions were transported toward the anode and accumulated there [17]. In the present study, nitrate and phosphate ions were the major cause for the increase in the EC of the anolyte because these anions move to the anode. Besides, cations like calcium, magnesium, and sodium move to the cathode, which determines the conductivity of the catholyte. Wiczonek *et al.* [32] reported higher EC in catholytes than anolytes in the EK process. During their experiment, the electrical conductivity increased in both wells, but three-fold levels were observed in the catholyte relative to the anolyte where copper, zinc, and nickel accumulated in the catholyte. In the present study, the magnitude order of solution conductivity followed the sequence of 0.615 > 0.307 > 0.123 mA/cm². The intensity of electromigration of existing species like phosphate, nitrate, calcium, sodium, and potassium determines the EC values. It is also due to the production of a large quantity of H⁺ in an anolyte which influences the conductivity of the catholyte by electroosmosis. Among all ionic species in the EK system, a high ratio of conductivity is contributed by H⁺ and OH⁻ due to their high molar ionic conductivities. It indicates that the solution conductance is dominated by water electrolysis. When the pH value is close to 7 at the initial period, the total concentration of H⁺ and OH⁻ is the lowest in comparison with other pH values. Therefore, the values of conductivity increase with decreasing pH at various current densities.

3.2. Potential of anode and cathode

The potential of the anode and cathode during the EK system is presented in Fig. 4. The initial OCP value of SS was about +75 mV vs SCE before starting the EK experiment. While impressing the current, the anode potential was in the range between 1.3 V and 1.5 V vs SCE while the cathode potential was in the range between -1.1 V and -1.5 V vs SCE. Hence, the material was scanned anodically (+1.5 V) and cathodically up to -1.5 V to find the electrochemical behavior of SS in various systems.

3.3. Weight loss of anode and cathode

The weight loss of the anode and cathode during the EK system at different current densities is presented in Fig. 5. The weight loss of the anode was in the following order 0.615 > 0.307 > 0.123 mA/cm² and the cathode corrosion rate was vice versa. It reveals that the application of a higher current protects the cathode surface and enhances anode cor-

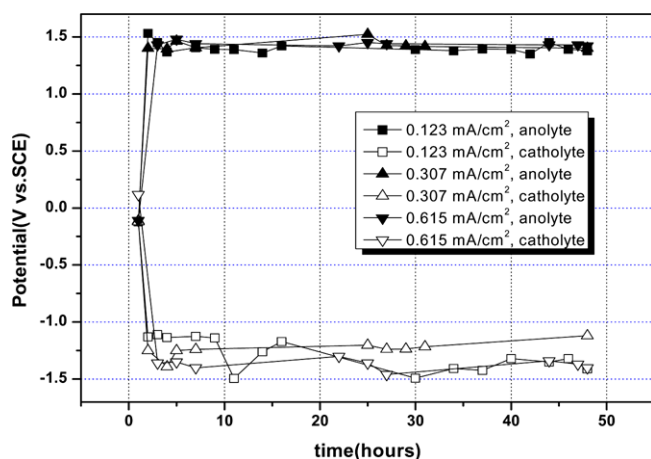


Fig. 4. Potentials measurements for anode and cathode of SS316 in EK system.

rosion. It indicates that electrode life can be reduced due to corrosion in the EK system.

3.4. Leaching of electrode components

Concentrations of chromium, iron, and nickel in the anolyte and catholyte in EK at various current densities are presented in Figs. 6(a), (b) and (c). The higher concentrations of chromium, nickel, and iron were estimated in the anolyte when compared to the catholyte. It indicates that toxic elements like chromium and nickel may travel to the cathode through the soil in the EK process by electroosmosis. Chromium compounds are highly toxic to plants and are detrimental to their growth and development. Although some crops are not affected by low Cr concentrations (3.8×10^{-4} μM), Cr is toxic to most high plants at $100 \mu\text{M kg}^{-1}$ dry weight [33]. The recommended limit for Cr concentration in water is set differently for Cr(III) ($8 \mu\text{g L}^{-1}$) and Cr (VI) ($1 \mu\text{g L}^{-1}$) [34].

3.5. Peroxide production

In the present study, 5 ppm, 10 ppm, and 25 ppm of peroxide were estimated at 0.123 mA/cm^2 , 0.307 mA/cm^2 , and

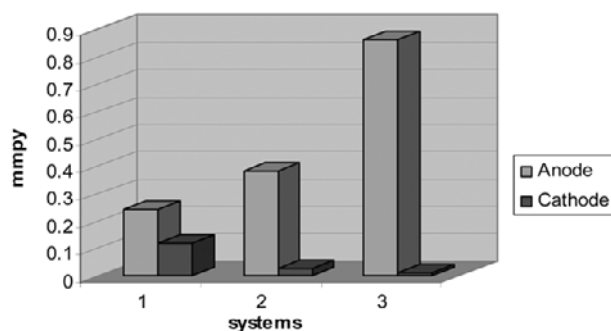


Fig. 5. Weight loss data for anode and cathode material of SS316L at different current densities in EK system. (System 1: 0.123 mA/cm^2 ; System 2: 0.307 mA/cm^2 ; System 3: 0.615 mA/cm^2).

0.615 mA/cm^2 , respectively, in anolyte. This observation supports the observation made by Ando and Tanaka [35] who proposed a new system for the simultaneous production of hydrogen and hydrogen peroxide by water electrolysis in the electroremediation process by employing carbon electrodes. The following chemical reaction was noticed by Ando and Tanaka [35] at the anode.

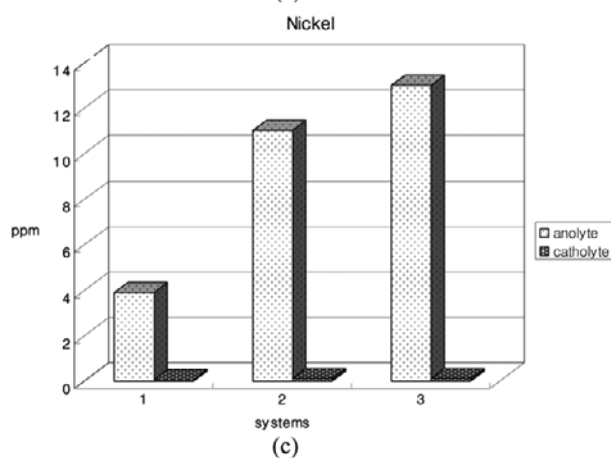
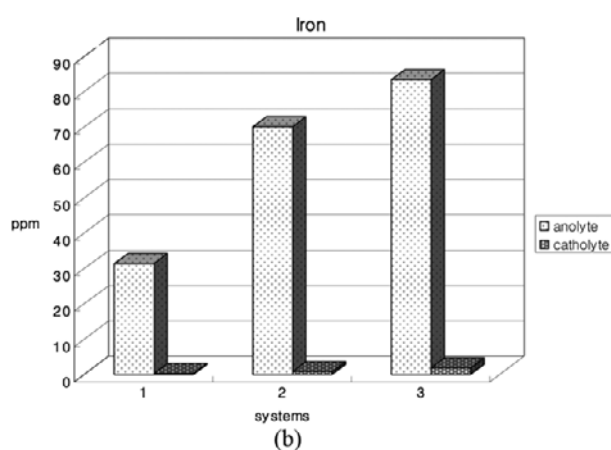
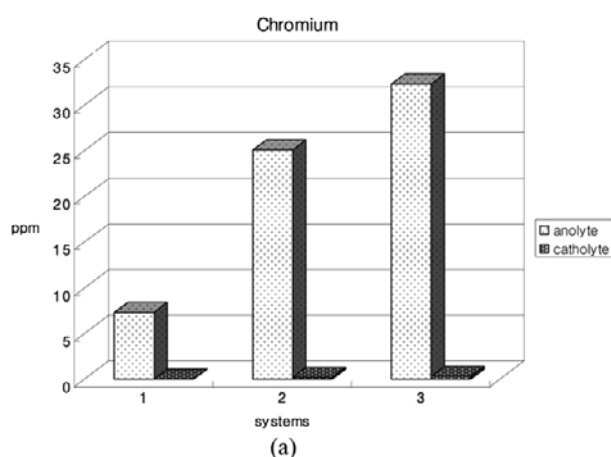
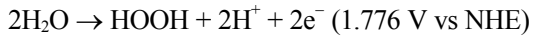


Fig. 6. Leaching of chromium (a), iron (b) and nickel (c) in anolyte and catholyte during EK process at different current densities (System 1: 0.123 mA/cm^2 ; System 2: 0.307 mA/cm^2 ; System 3: 0.615 mA/cm^2).



They also suggested that the anode material promotes the hydrogen peroxide production rate and that inhibition of the oxygen evolution reaction rate is required in order to realize the proposed system. Recently, the present authors also noticed 25 ppm of peroxide production by using a titanium substrate insoluble anode (TSIA) at 1.35 V vs SCE. It can be assumed that the H_2O_2 so generated can be coupled with Fe^{2+} to produce the Fenton's reagent [31] for degradation of TOC (total organic content) in the soil at the anodic area [36]. The disadvantage is that the H_2O_2 will accumulate at the anode solution interface and may be partially decomposed protons at a high concentration leading the production of the maximum amount of hydroxyl radicals. It is also possible that due to the electroosmotic process, the peroxide may influence the cathode compartment and enhance the degradation of organics present in the soil [37-39]. Hence, the peroxide concentration should be minimized in the EK system to avoid degradation of the TOC by selection of a better anode for agricultural soil.

3.6. Electrochemical studies

3.6.1. Potential measurements

Figure 7 shows potential measurements with time for SS316L in acidic, neutral, and alkaline systems. The OCP of SS316L in a neutral condition was in the range between -30 mV vs SCE and $+50 \text{ mV vs SCE}$. The OCP for SS316L in the acidic and alkaline systems was $+0.370 \text{ mV}$ and -185 mV , respectively. It indicates that the addition of acetic acid enhances passivity of stainless steel by shifting the potential to the positive side. Sekine *et al.* [40] also reported a rapid increase in potential upon immersion of SS316L in a solution of acetic acid (1-99.96%). Turnbull *et al.* [41] suggested that the shifting of potential to the positive side in SS316L is due to the molybdenum which improves the passivity of

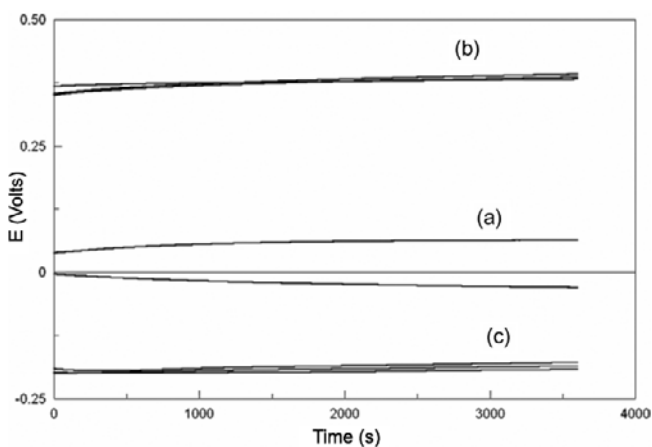


Fig. 7. Potential measurements for SS316 in neutral (a), acidic (b) and alkaline pH (c) conditions of soil extract.

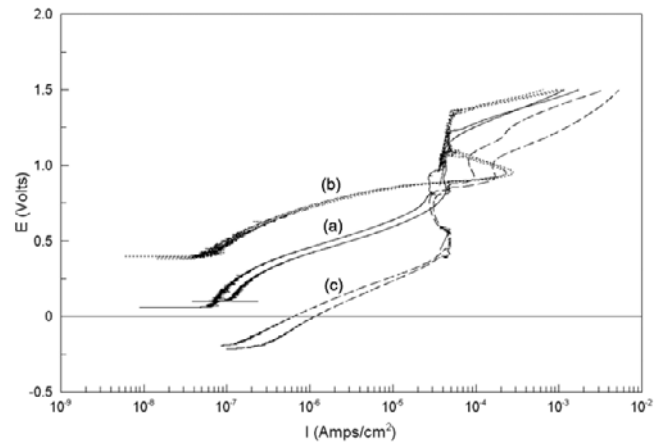


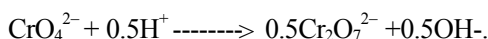
Fig. 8. Anodic polarization for SS316 L in neutral (a), acidic (b) and alkaline (c) pH conditions of soil extraction.

material. However, chromium is expected to influence the protectiveness of the film as the corrosion potential of the pure chromium stabilized at a value of 0.4 V vs SCE [40]. Turnbull *et al.* [41] also suggested that Fe in the steel does not seem to play any role in the passivation process of SS316L in acetic acid solutions.

3.6.2. Anodic polarization

Anodic polarization curves for the SS316L in neutral, acidic, and alkaline soil extracts are shown in Fig. 8. The scans have the same general features and are characterized by the appearance of active, passive, and transpassive regions before oxygen evolution. When the potential moves toward more anodic, the current density starts to increase again, forming a transpassive region before oxygen evolution. From an industrial point of view, transpassive dissolution is an important issue on limiting the service life of electrodes. The current rises suddenly without any sign of oxygen evolution denoting breakdown of the passive layer, when the polarization potential reaches a certain critical potential. The i_p (current density in the passive region) of the SS 316L in the neutral soil system was about $3 \times 10^{-5} \text{ A/cm}^2$ where the breakdown potential was 1.2 V vs SCE . The passivity range was from 0.750 V to 1.2 V in the neutral system. The i_p of the SS316L in the acetic acid system (pH 2.5) was about $4 \times 10^{-5} \text{ A/cm}^2$ whereas the breakdown potential was 1.35 V . The passivation potential range was between 1.0 V and 1.35 V whereas passivation started at $+0.9 \text{ V}$. In the alkaline system, passivation started at $+190 \text{ mV}$ where the i_p of the SS was about $3 \times 10^{-5} \text{ A/cm}^2$. Secondary passivation was also noticed in the alkaline system. The first breakdown potential was $+600 \text{ mV}$ and the second was about $+810 \text{ mV}$. The nature of the curve reveals that acetic acid improves the passivity of stainless steel when compared to other systems. The passive film of the stainless steel contains three oxides viz. ferric oxide, chromium oxide, and nickel oxide. Most iron containing alloys are dominated by ferric oxides [42]. The

nature and composition of the passive films formed on stainless steel, especially their protective nature, are dependent on the formation conditions. The stable passive film formed on the SS316L is heterogeneous. These films are described by a bilayer structure, composed essentially of a chromium hydroxide, $\text{Cr}(\text{OH})_3$, outer layer and a mixed inner layer of chromium and iron oxides, enriched in chromium [43]. In the present study, enhanced anodic current density was observed in the active to passive transition region at +0.9 V in the acetic acid system. There was a sharp increase in current at about +1.2 V, possibly due to either oxidation of the Cr^{3+} in the passive film to Cr^{6+} species, or oxygen evolution, or a combination of both in the acetic acid aqueous solutions [44]. Liu *et al.* [45] noticed that the corrosion rate decreased with increasing chromium and molybdenum contents. It is also well known that for a given chromium content in SS the addition of molybdenum has a strong beneficial influence on passivity in the chloride solution. They also suggested that Cr^{3+} and MO^{2+} oxides are highly stable in a HAC solution. The nature of the passive [46] film was explained by assuming that the reaction of the SS includes the irreversible transformation of chromate formed according to soluble dichromate species, which are stable in the pH range 2-6:



Besides, it also can be claimed that the breakdown potential indicates the oxidation of ferric and chromium present on the oxide film of the SS316L in acid, neutral, and alkaline conditions [47,48].

3.6.3. Cathodic polarization

Figure 9 shows cathodic polarization for the SS316L in different systems viz. neutral, acidic, and alkaline pH. In the neutral system, the current slowly increased from -300 mV along with increasing the potential to a negative side. A broad peak from -500 mV/SCE to -900 mV/SCE was noticed. In the alkaline system, the current increased with a negative

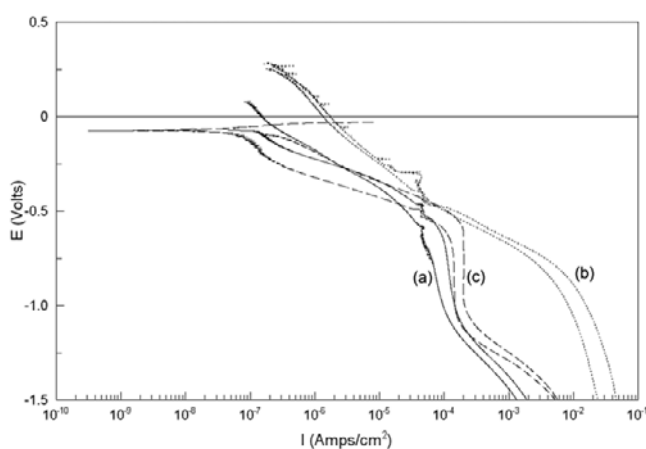


Fig. 9. Cathodic polarization for SS316L in neutral (a), acidic (b) and alkaline (c) pH conditions of soil extraction.

potential from -500 mV to -700 mV. These peaks can be explained due to the chromium reduction peak [29,30]. In the acidic system, the current also increased slowly along with negative potential. The increased current trend was noticed above -600 mV at pH 2. It is due to oxygen reduction. The increased current is due to the electrolysis of acetic acid.

3.7. XPS characterization of the outermost surface film

To better understand the elemental composition of the passive film on the SS316L anode and cathode surfaces in an EK system, a detailed XPS study was carried out on the outermost layers of the SS316L. After finishing the EK study in 48 h at 0.615 mA/cm^2 , the anode and cathode were removed and characterized by XPS to acquire the Fe 2p, Cr 2p, O 1s, Ca, Mg. The spectra obtained from the passive film of the anode and cathode after 48 h of exposure to the EK system are shown in Figs. 10(a) and (b). Five peak components on the cathode at binding energies (i.e., B.E.s) of 706.9, 708.3, 709.5, 711.0, and 712.2 correspond to the metallic Fe, Fe_3O_4 , FeO, Fe_2O_3 , and FeOOH, respectively. It indicates that Fe, Fe^{2+} , Fe^{3+} , and FeOOH were the predominant species on the cathode. The presence of a large number of species may be due to the reduction of FeOOH on the oxide film of the SS316L. Fe_2O_3 is the major dominant species on the anode of the SS316L. Lee *et al.* [49] suggested that ferric oxide changed from FeO to Fe_2O_3 when immersion time was increased in a Cl⁻/Br⁻ solution. Chromium peak components at B.E.s of 573.95, 573.95, 574.9 (Cr), 576.9 (Cr^{3+}), 578.3 (CrO_3), and 579.4 (CrO_4^{2-}) were measured. The domination

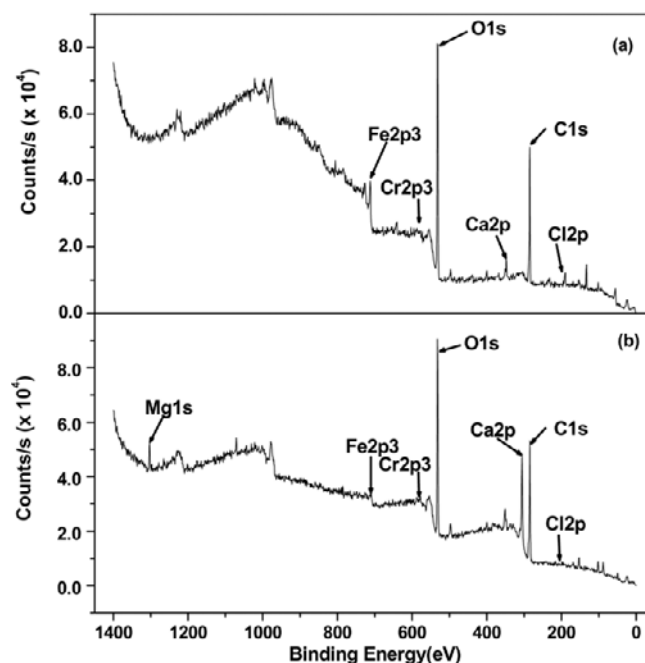
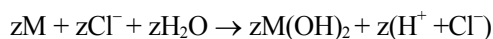


Fig. 10. XPS survey of SS316L in EK process (a-anode, b-cathode).

enhances the reduction of chromium and iron. In the present study, the value of electroosmosis was 60 ml/day at 0.615 mA/cm². Hence, the chloride travels from the anode chamber to the cathode chamber and attacks the metal surface. It is well known that during cathodic protection, the presence of a protective oxide film undergoes reduction. The cathodic surface of SS316L has a significant quantity of Fe²⁺ and Fe³⁺ and reduced species of chromium. The present authors also strongly believe that the adsorption of porous calcium and magnesium oxide film encourages the entry of Cl⁻ through the porous film. It is possible that the reduced species attracts the negative species of chloride and forms as metallic chlorides on the cathodic surface. Shang and Lo [57] did not detect Fe³⁺ at the cathode even though corrosion was expected at the anode, which was probably because Fe³⁺ formed at the steel anode was transported to the bottom cathode by electromigration and precipitated to insoluble iron-hydroxide (Fe(OH)₃). Hence, it can be claimed that the deposit on the cathode surface may create differential aeration cells which is a favorable environment for pitting corrosion. Besides, H⁺ also travels from the anodic to cathodic chamber through electroosmosis [21]. The fact is that the mobility of the protons under the electrical field is about two times faster than hydroxyl ion mobility, which is a factor that can make it dominate a system that contains both [4]. The formation of an autocatalytic reaction to form hydrochloric acid on a metal surface may encourage the pit formation on a cathodic surface.



Zucchi *et al.* [58] observed that stainless steel suffered hydrogen embrittlement when cathodically polarized in deaerated artificial seawater. They observed a calcareous deposit at -1.2 V vs SCE. Although the solution pH was maintained at about 6.5 by adding HCl, the pH at the metal/solution interface could reach high enough values to precipitate Mg(OH)₂. They concluded that SS was susceptible to hydrogen embrittlement in a deaerated pH 6.5 when cathodically protected at -0.9 V/SCE. In the present study, pittings were also noticed on the anodic surface of the SS316L. It is due to the dissolution of oxides at the transpassive region in all pH systems. Hence, the authors strongly believe that SS316L releases chromium and iron in the soil by corrosion and contaminates the soil.

The behavior of cathodically protected stainless steel in natural or artificial seawater has not been frequently investigated. Though many investigators used SS as a cathode material [18-26], nobody has considered the electrochemical behavior of cathode SS electrodes in the EK process. In literature, nobody has mentioned the "grade of stainless steel" used in the EK system. Isosaari *et al.* [59] used stainless steel as electrodes in electroremediation of creosote contaminated clay and they noticed that corrosion of the SS plate elec-

trodes could have acted as an additional source of Fe. They also mentioned that the concentrations of Cr, Ni, and Mo were present in the stainless steel electrodes, which were not markedly elevated in the clay. Besides, they noticed the presence of Cr, Ni, and Mo in the anolyte and catholyte and suggested that the corroded components migrated toward the cathode from the anode. Hence, investigators believe that this study may create awareness about electrochemical behavior of SS on electroremediation to environmental engineers.

Raats [60] did EK dewatering of waste sludge by stainless steel electrodes in a pilot scale. Due to the electrochemical dissolution of the anode, titanium coated with iridium oxide as an electrode material was used and dissolution was suppressed effectively. Chen [61] suggested that graphites and lead oxide are among the most common insoluble anodes used in electrofloatation. They are also cheap and easily available, but both showed high O₂ evolution overpotential and low durability. Besides, in lead there exists a possibility to generate highly toxic Pb²⁺, leading to severe pollution. A few researchers reported the use of Pt or Pt-plated meshes as anodes [62,63]. They are much more stable than graphite and lead oxide. However, the known high cost makes large scale industrial application impracticable. The well known TiO₂-RuO₂ types of dimensionally stable anodes (DSA) discovered by Beer [64] which possess high quality for chlorine evolution but their service life is short for oxygen evolution. In the last decade, IrO_x presents a service life about 20 times longer than that of the equivalent RuO₂ (70 %). Hence, the selection of an electrode should be made on the basis of pollutants in the soil and electrochemical behavior of the electrode in the polluted environment.

4. CONCLUSIONS

Stainless steel is used as either a cathode or an anode in an EK system on removal of pollutants in soil and water environments. The corrosion behavior of an electrode in an EK system has not been considered. In the present study, leaching of chromium, nickel, and iron has been noticed in the catholyte and anolyte during the EK process. The weight loss of an anode is higher than a cathode in the EK process, which reduces the life of the electrode. Peroxide production in the EK process is also a negative effect on distribution of organic content in the agricultural soil. The impressed current in EK encourages the shifting of potential to a transpassive region and enhances corrosion if SS is used as an anode. The addition of acetic acid improves the passivity of the SS electrode. The XPS study indicates the presence of reduced/oxidized species of chromium and iron on the cathode and anode. Besides, the adsorption of calcium and magnesium has been noticed on the cathode only. Pitting has been noticed on both the anode and cathode and concludes

that the formation of an autocatalytic reaction by chloride on the metal surface may encourage the pit formation on the cathodic surface. The pitting on the cathodic surface is correlated with the movement of H^+ from the anode to the cathode chamber by electroosmotic flow in the EK process. Hence, the application of stainless steel as an electrode in electroremediation technology for agricultural soil and drinking water is questionable.

ACKNOWLEDGEMENTS

S. Maruthamuthu is grateful to the Korean Federation of Science and Technology Societies, Korea, for the award of a Brain Pool Fellowship to carry out this work and also thanks Central Electrochemical Research Institute (CSIR), India, for granting deputation to KERI, South Korea. The authors thank Dr. L. Y. Kim, the soil physics laboratory, and the National Institute of Agricultural Science and Technology for analyzing the salts ions and helping in the collection of soil.

REFERENCES

1. J. Virkutyte, M. Sillanpaa and P. Latostenmaa, *Sci. Total Environ.* **289**, 97 (2002).
2. Y. B. Acar and A. N. Alshawabkeh, *Environ. Sci. Tech.* **27**, 2638 (1993).
3. K. Reddy, M. Donahue and R. Sasaoka, *Air. Waste. Manage. Asso.* **49**, 823 (1999).
4. D. B. Sogorka, H. Gabert and B. J. Sogorka, *Hazard. Ind. Wastes.* **30**, 673 (1998).
5. L. Van Cauwenberghe, *Electrokinetics: Technology overview Report*, p.1-17, Ground water Remediation Technologies Analysis Centre (1997).
6. Benazon, N, *Hazard Mater Mange* **7**, 10 (1995).
7. D. M. Zhou, C-F. Deng, L. Cang, and A. N. Alshawabkeh, *Chemosphere* **61**, 519 (2005).
8. Y. B. Acar, R. J. Gale, A. N. Alshawabkeh, R. J. Marks, S. Puppala, M. Bricka, and R. Parker, *J. Hazar. Mater.* **40**, 117 (1995).
9. B. Komilovich, N. Mishchuk, K. Abbruzzese, G. Pshinko, and R. Klishchenko, *Colloids and Surfaces A: Physico Chem. Eng. Aspects.* **265**, 114 (2005).
10. A. Giannis and E. Gidaracos, *J. Hazar. Mater. B.* **123**, 163 (2005).
11. C. Vereda-Alonso, J. M. Rodríguez-Maroto, R. A. García-Delgado, C. Gómez-Lahoz, and F. García-Herruzo, *Chemosphere* **54**, 895 (2005).
12. P. Wieberen, *European Patent Specification*, Publication Number 0312174 B1 (1992).
13. R. F. Probstein, *Proc. 12nd Annual USEPA-RREL, Research Symposium*, EPA/600/R-94/011 p. 210 (1994).
14. S. J. Yuan and S. O. Pehkohen, *Colloids and Surfaces B: Biointerfaces* **59**, 87 (2007).
15. S.-Oh. Kim, W. S. Kim, and K. W. Kim, *Environ. Geochem. Hlth.* **27**, 443 (2005).
16. Q. Luo, X. Zhang, H. Wang, and Y. Qian, *Chemosphere* **59**, 1289 (2005).
17. K. Manokarrajah and R. S. Ranjan, *Eng Geol.* **77**, 263 (2005).
18. S. Micic, J. Q. Shang, and K. Y. Lo, *Can. Geotech. J.* **40**, 949 (2007).
19. T. Paillet, F. Moreau, P. O. Grimcud, and G. Touchard., *IEEE Transactions on Dielectrics and Electrical Insulation* **7**, 693 (2000).
20. P. Isoasaari, R. Piskonen, P. Ojala, S. Vorpro, K. Eilola, E. Lehmus, *J. Hazar. Mater.* **144**, 538 (2007).
21. J. H. Chang and Y. C. Loo, *J. Hazar. Mater. B.* **129**, 186 (2006).
22. M. Elecktutowicz and S. Habibi, *Can. J. Civil. Eng.* **32**, 164 (2005).
23. G. Kristina and V. Saulius, *Geologija.* **57**, 55 (2006).
24. N. A. Alshawabkeh, P. E. Asce, and R. M. Bricka, D. B. Gent, *J. Geotech and Geoenviron. Eng.*, 283 (2005).
25. D. B. Gent, R. M. Brick, A. N. Alshawabkeh, L. S. Larson., G. Falian, and S. Granade, *J. Hazar. Mater.* **110**, 53 (2004).
26. J. L. Niqui-Arroyo, M. Bueno-Montes, R. Posado-Baquero, and J. J. Ortega-calro, *Environ. Pollution*, **142**, 326 (2006).
27. S. Vasudevan, G. Sozhan, S. Ravichandran, J. Jeyaraj, J. Lakshmi, and S. M. Sheela, *Ind. Eng. Chem. Res.* **47**, 2018 (2008).
28. J. T. Hamed and A. Bhadra, *J. Hazar. Mater.* **55**, 279 (1997).
29. R. S. Treseder, R. Baboian, and C. G. Munger, *NACE Corrosion Engineer's Reference Book*, p. 78, NACE, Houston, Texas (1991).
30. S. Maruthamuthu, S. Sathiyarayanan, R. Palaniappan, and N. Palaniswamy, *Corrosion 2002*, NACE International, Houston, Texas (2002).
31. G. Chen, *Sep. Purif. Technol.* **38**, 11 (2004).
32. S. Wiczorek, H. Weigand, M. Schmid and C. Marb, *Eng. Geol.* **77**, 203 (2005).
33. A. K. Shanker, C. Cervantes, H. Loza-Tavera and S. Avudainayagam, *Environ. Int.* **31**, 739 (2005).
34. P. Chandra, S. Sinha and UN. Rai, *Phytoremediation of Soil and Water Contaminants* (eds., E. L. Kruger, T. A. Anderson, J.R), p. 274, ACS Symposium Series, 1.664, Washington DC, American Chemical Society (1997).
35. Y. Ando and T. Tanaka, *Int. J. Hydrogen Energ.* **29**, 1349 (2004).
36. J. Virkutyte and V. Jegatheesan, *Bioresource Technol.* **100**, 2189 (2009).
37. E. Brillas, R. Sauleda and J. Casada, *J. Electrochem. Soc.* **144**, 2374 (1997).
38. E. Brillas, R. Sauleda and J. Casado, *J. Electrochem. Soc.* **145**, 759 (1998).
39. E. Brillas, E. Mur, R. Sauleda, L. Sanchez, F. Peral, X. Domenech, and J. Casado, *Appl. Catal. B: Environ.* **16**, 31

- (1998).
40. I. Sekine, S. Hatakeyama and Y. Nakazawa, *Electrochim. Acta* **32**, 915 (1987).
 41. A. Turnbull, M. Ryan, A. Willetts and S. Zhou, *Corros. Sci.* **45**, 1051 (2003).
 42. N. Sato, *Passivity of metals*, (eds., R. P. Frankenthal and J. Kanger) p. 29, Electrochemical Society, Princeton, NJ (1978).
 43. S. S. El-Egamy and W. A. Badaway, *J. Appl. Electrochem.* **34**, 1153 (2004).
 44. A. J. Invernizzi, E. Sivieri, and S. Trasatti, *Mat. Sci. Eng. A* **485**, 234 (2008).
 45. G. Q. Liu, Z. Y. Zhu, E. H. Han, and C. L. Zeng, *Corrosion* **57**, 730 (2001).
 46. I. Betova, M. Bojinov, T. Laitinen, K. Makela, P. Pohjanne, and T. Saario, *Corros. Sci.* **44**, 2699 (2002).
 47. M. Pourbaix, *Atlas of Electrochemical Equilibria in Aqueous Solution*, NACE, Houston (1974).
 48. S. A. M. Rafeey, M. Taha, and A. Malak, *Appl. Surf. Sci.* **242**, 114 (2005).
 49. S. U. Lee, J. C. Ahn, D. H. Kim, S. C. Hong, and K. S. Lee, *Mat. Sci. Eng. A* **434**, 155 (2006).
 50. H. Milosev and H. Strehblow, *J. Biomed. Res.* **52**, 404 (2000).
 51. A. Atrens and B. Baroux, *J. Electrochem. Soc.* **144**, 3697 (1997).
 52. A. S. Tselesh, *Thin Solid Films* **526**, 6253 (2008).
 53. M. Eashwar, G. Subramanian, P. Chandrasekaran, S. T. Manickam, S. Maruthamuthu, and K. Balakrishnan, *Bio-fouling* **8**, 303 (1995).
 54. C. D. Wagner, A. V. Naumkin, A. Kraut-vass, J. W. Allison, C. J. Powell, and J. R. Rumble, Jr., *NIST X-ray Photoelectron Spectroscopy Database: NIST Standard Reference Database: NIST Standard Reference Database 20*, Version 3.4 (Web version), <http://srdata.nist.gov/XPS/2003> (2003).
 55. D. C. Catherine, S. Haskouri, and H. Cachet, *Appl. Surf. Sci.* **253**, 5506 (2007).
 56. S. T. Lohner, D. Becker, H. Schell, T. Angenstein, C. Weidlich, K.-M. Mangold, K.-M. Juttner, and A. Tiehm, *6th Symposium on Electrokinetic Remediation (EREM 2007)*, Paper No. S41, Vigo, Spain. (2007).
 57. J. Q. Shang and K. Y. Lo, *J. Hazar. Mater.* **55**, 117 (1997).
 58. F. Zucchi, V. Grassi, C. Monticelli, and G. Trabanelli, *Corros. Sci.* **48**, 522 (2006).
 59. M. H. M. Raats, A. J. G. van Diemen, J. Lavén, and H. N. Stein, *Colloids and Surfaces A: Physicochem. Eng. Aspects* **210**, 231 (2002).
 60. P. Jsosaari, R. Piskonen, P. Ojala, S. Voipo, E. K. Eilola, E. Lehmus, and M. Itavaara, *J. Hazar. Mater.* **144**, 538 (2007).
 61. G. Chen, *Sep. Purif. Technol.* **38**, 11 (2004).
 62. D. R. Ketkar, R. Mallikarjunan and S. Venkatachalam, *Int. J. Miner. Proc.* **31**, 127 (1991).
 63. C. P. C. Poon, *J. Hazard. Mater.* **55**, 159 (1997).
 64. H. B. Beer, *Electrode and Coating Therefore*, US patent 3,632,498 (1972).